

PAPER

Imaging and dosimetric characteristics of ^{67}Cu

To cite this article: Michael J Merrick *et al* 2021 *Phys. Med. Biol.* **66** 035002




View the [article online](#) for updates and enhancements.

You may also like

- [The on-line low temperature nuclear orientation facility NICOLE](#)
T Ohtsubo, S Roccia, N J Stone et al.
- [Correlation and spectrum shape measurements in \$\beta\$ -decay probing the standard model](#)
N Severijns
- [14.77 MeV neutron-induced nuclear reaction cross sections for zinc, yttrium, and molybdenum targets](#)
T.S. Ganesapandy, G.T. Bholane, S.H. Patil et al.



PAPER

Imaging and dosimetric characteristics of ^{67}Cu Michael J Merrick^{1,2} , David A Rotsch³ , Ashok Tiwari^{1,4}, Jerry Nolen³, Thomas Brossard⁵, Jeongseog Song³, Thaddeus J Wadas¹, John J Sunderland^{1,4} and Stephen A Graves^{1,2,6,*} ¹ Department of Radiology, University of Iowa, Iowa City, IA, United States of America² Department of Biomedical Engineering, University of Iowa, Iowa City, IA, United States of America³ Physics Division, Argonne National Laboratory, 9700 S. Cass Ave, Lemont, IL 60439, United States of America⁴ Department of Physics, University of Iowa, Iowa City, IA, United States of America⁵ Chemical and Fuel Cycle Technologies Division, Argonne National Laboratory, 9700 S. Cass Ave, Lemont, IL 60439, United States of America⁶ Department of Radiation Oncology, University of Iowa, Iowa City, United States of America

* Author to whom any correspondence should be addressed.

E-mail: stephen-graves@uiowa.edu**Keywords:** radiopharmaceutical therapy, theranostics, copper, SPECT/CTSupplementary material for this article is available [online](#)

RECEIVED

8 July 2020

REVISED

2 November 2020

ACCEPTED FOR PUBLICATION

13 November 2020

PUBLISHED

25 January 2021

Abstract

In recent years the use of beta-emitting radiopharmaceuticals for cancer therapy has expanded rapidly following development of therapeutics for neuroendocrine tumors, prostate cancer, and other oncologic malignancies. One emerging beta-emitting radioisotope of interest for therapy is ^{67}Cu ($t_{1/2}$: 2.6 d) due to its chemical equivalency with the widely-established positron-emitting isotope ^{64}Cu ($t_{1/2}$: 12.7 h). In this work we evaluate both the imaging and dosimetric characteristics of ^{67}Cu , as well as producing the first report of SPECT/CT imaging using ^{67}Cu . To this end, ^{67}Cu was produced by photon-induced reactions on isotopically-enriched ^{68}Zn at the Low-Energy Accelerator Facility (LEAF) of Argonne National Laboratory, followed by bulk separation of metallic ^{68}Zn by sublimation and radiochemical purification by column chromatography. Gamma spectrometry was performed by efficiency-calibrated high-purity germanium (HPGe) analysis to verify absolute activity calibration and establish radionuclidic purity. Absolute activity measurements corroborated manufacturer-recommended dose-calibrator settings and no radionuclidic impurities were observed. Using the Clinical Trials Network anthropomorphic chest phantom, SPECT/CT images were acquired. Medium energy (ME) SPECT collimation was found to provide the best image quality from the primary 185 keV gamma emission of ^{67}Cu . Reconstructed images of ^{67}Cu were similar in quality to images acquired using ^{177}Lu . Recovery coefficients were calculated and compared against quantitative images of $^{99\text{m}}\text{Tc}$, ^{177}Lu , and ^{64}Cu within the same anthropomorphic chest phantom. Production and clinical imaging of ^{67}Cu appears feasible, and future studies investigating the therapeutic efficacy of ^{67}Cu -based radiopharmaceuticals are warranted.

1. Introduction

Radiopharmaceutical therapy has expanded rapidly in recent years, with several new and exciting oncologic targets (Forrer *et al* 2007, Grozinsky-Glasberg and Gross 2012). Approval of ^{177}Lu -DOTATATE in the U.S. for treatment of neuroendocrine tumors in 2017 marked the first radiometal-based peptide radiotherapeutic, however radiometal-based PSMA-targeted agents for prostate cancer are widely expected to be approved in the near future (Kaltsas *et al* 2005, Mitra 2018). The primary goal in radiopharmaceutical therapy, as with other approaches to radiotherapy, is to deliver a therapeutic level of absorbed dose to the target while limiting exposure to healthy tissue. This objective defines the desirable physical properties of a theranostic radioisotope, in addition to the biochemical properties of a targeting ligand. Both beta- and alpha-emitting radioisotopes have shown success for improving patient outcomes, however further work is needed in

improving radiopharmaceutical stability and overall therapeutic ratio (Lubberink *et al* 2020). Increasing the availability and diversity of therapeutic radioisotopes may enable these advances in radiopharmaceutical design.

Recently, ^{67}Cu ($t_{1/2}$: 2.6 d) has become available in the U.S., through the Department of Energy Isotope Program (DOE-IP), in quantities and purities that are sufficient for medical research applications. Researchers at Argonne National Laboratory have developed a production route that uses high-energy photon-induced reactions on isotopically enriched ^{68}Zn targets (Ehst *et al* 2012; Ehst and Bowers 2013, Ehst and Willit 2016). Prior production methods used by other groups include the use of cyclotrons to irradiate ^{68}Zn with medium-energy protons (Schwarzbach *et al* 1995). This method of ^{67}Cu —produced by (p, 2p) nuclear reactions—has relatively low yield and suffers from prominent radionuclidic impurities including ^{62}Zn , ^{67}Ga , ^{65}Zn , ^{55}Co , ^{58}Co and ^{57}Ni (Schwarzbach *et al* 1995). The burdensome radiochemical isolation procedure needed to purify ^{67}Cu produced by this path, combined with low production rates, has prevented availability of this otherwise promising radioisotope.

Copper-67, has been long sought after as a desirable therapeutic companion to the widely utilized PET isotope ^{64}Cu ($t_{1/2}$: 12.7 h). The well-established coordination chemistry of copper and established radiochemistry for ^{64}Cu allows for immediate incorporation of ^{67}Cu in a wide variety of targeting ligands—including peptides, antibodies, proteins, nanoparticles, and other biologically relevant small molecules (Moi *et al* 1985, Linder and Hazegh-Azam 1996, Lewis *et al* 1999a, 1999b, Bass *et al* 2000, Anderson and Ferdani 2009). Copper-67 emits beta particles with a mean and maximum energy of 141 keV and 562 keV respectively, which is consistent with the emissions of other commonly used therapeutic radioisotopes (e.g. ^{177}Lu and ^{131}I). Along with 100% beta emission, ^{67}Cu also emits a 185 keV gamma in 49% of decays, which is suitable for single photon emission computed tomography (SPECT). The favorable combination of established bioconjugate chemistry, half-life, gamma, and beta emissions are what make ^{67}Cu attractive as a therapeutic and potentially theranostic radioisotope (Sun and Anderson 2004). With that said, there are currently no literature reports of therapy with, or single-photon imaging of, ^{67}Cu .

To facilitate the continued development of this promising radioisotope, we have evaluated the characteristics of ^{67}Cu in a clinical setting. In particular we (A) assessed the radionuclidic purity of the final ^{67}Cu product; (B) compared the physical dosimetric characteristics of ^{67}Cu with other relevant beta-emitting radionuclides using Monte Carlo simulations; and (C) evaluated the SPECT/CT imaging characteristics of ^{67}Cu in comparison with other relevant radioisotopes on pre-clinical and clinical scanners.

2. Methods and materials

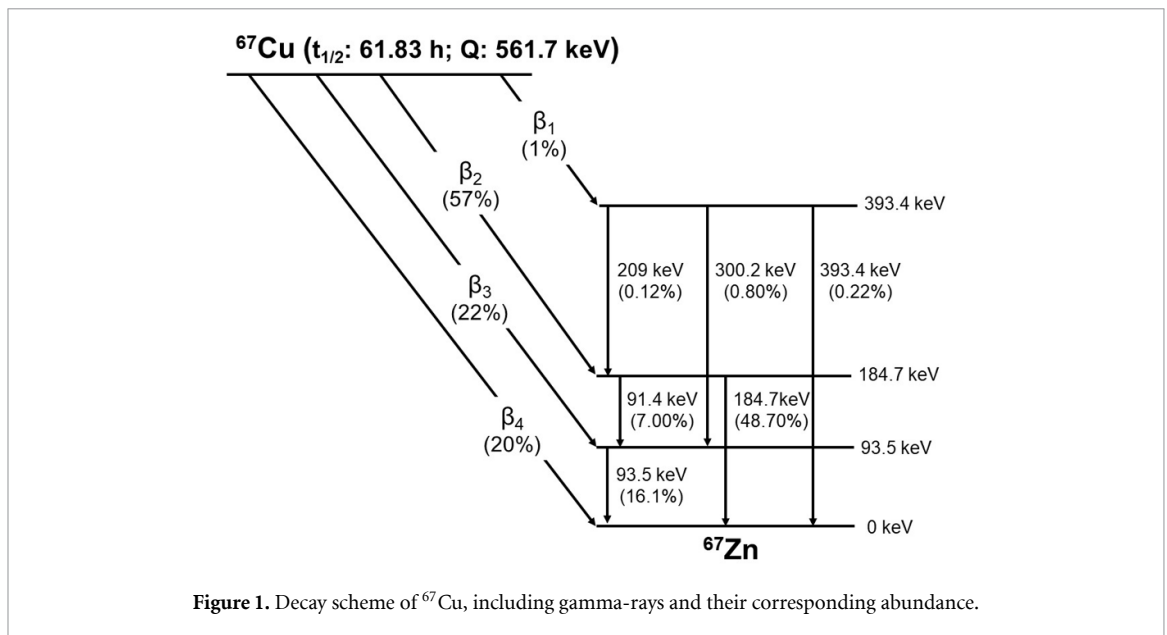
2.1. ^{67}Cu production

Copper-67 was produced at the Argonne National Laboratory Low Energy Accelerator Facility (LEAF) via the $^{68}\text{Zn}(\gamma, p)$ nuclear reaction. Bremsstrahlung radiation was produced by impinging a 40 MeV electron beam with an average power of 18.2 kW onto a water-cooled tantalum conversion target. An isotopically enriched ^{68}Zn metal ingot target (55.5 g) was placed behind and proximal to the Bremsstrahlung conversion target, and the target was irradiated for a period of 53.5 h.

Produced ^{67}Cu was isolated from the bulk ^{68}Zn matrix by a dry sublimation technique (Marceau *et al* 1970, Ehst and Bowers 2013, Ehst and Willit 2016). The copper-rich residue was digested with hydrochloric acid (8 M, 8 ml) and concentrated nitric acid (1.0 ml) under gentle heating. This solution was evaporated to dryness to remove HNO_3 . The resulting residue was cooled to room temperature, was re-dissolved with HCl (8 M, 8 ml), and then passed through a gravity-fed anion exchange column (Dowex[®] AG 1 \times 8 HCl, 100–200 μm , 10 ml bed volume). The column was washed with HCl (8 M, 8 ml) and the product was eluted with HCl (2.5 M, 16 ml). The eluent fractions were combined and passed through a polishing column collected and evaporated to dryness. The residue was reconstituted with HCl (0.05 M, 1.0 ml). The final product was sampled and analyzed by inductively-coupled mass spectroscopy (ICP-MS) and high-purity germanium spectroscopy (HPGe). The apparent molar activity was determined by titrating small portions of the final product with TETA (1,4,8,11-tetraazacyclotetradecane-1,4,8,10-tetraacetic acid) and DOTA (1,4,7,10-tetraazacyclododecane-1,4,7,10-tetraacetic acid).

2.2. HPGe calibration

Gamma spectrometry was performed using a calibrated HPGe detector (Ortec GEM20P4-70). HPGe efficiency calibration was performed using NIST-traceable sources of ^{241}Am , ^{57}Co , ^{137}Cs , ^{60}Co and ^{152}Eu (3% Uncertainty, Eckert & Ziegler). Spectral analysis was performed using the SAMPO code, which utilizes a sophisticated peak fitting algorithm (Routti 1969, Aarnio *et al* 1995, 2001). Efficiency calibration was performed by linear least squares regression.



2.3. Radionuclidic purity

Gamma spectrometry was performed to confirm the radionuclidic purity of produced ^{67}Cu . One impurity of interest is ^{67}Ga due to its presence in other production routes, such as (p, 2p) nuclear reactions using medium-energy cyclotrons. However, it has never been observed during gamma-induced reactions and is not expected at the energies used during the irradiations. Detection of ^{67}Ga can be challenging to detect by gamma spectrometry due to gamma emission energies that overlap with what is emitted by ^{67}Cu (91, 93, 185, 209, 300, 394 keV). With that said, the branching ratios for each emission differ between ^{67}Cu and ^{67}Ga , so it is necessary to accurately measure branching ratios to verify the absence of ^{67}Ga (Dasgupta *et al* 1991, Schwarzbach *et al* 1995). Copper-67 decays 100% through β^- decay, of the four possible β^- decay routes three of which are followed by immediate gamma emission 91.4 keV (7.00%), 93.5 keV (16.10%), 184.7 keV (48.70%), 209.0 keV (0.12%), 300.2 keV (0.80%) and 393.4 keV (0.22%) (figure 1). Experimental branching ratios were assessed by efficiency-calibrated gamma spectrometry, followed by normalization to the primary 185 keV emission.

2.4. Absolute activity verification

Absolute activity quantification was performed by efficiency-calibrated HPGe spectrometry as a method of validating manufacturer-specified dose calibrator settings for ^{67}Cu (University of Iowa—Biodex AtomLab 500 dose calibrator, dial setting 43.6; Argonne National Laboratory—Biodex AtomLab 500 dose calibrator, dial setting 43.6). An aliquot was measured by dose calibrator at Argonne National Laboratory prior to shipping, and the same aliquot was measured at the University of Iowa upon receipt. A quantitative dilution of this aliquot was then prepared and assayed by HPGe. An uncertainty-weighted average of activities determined from each ^{67}Cu photopeak was then used to generate an absolute activity measurement, against which the dose calibrator measurements could be compared.

2.5. Pre-clinical $\mu\text{SPECT/CT}$ imaging

To evaluate the image quality that could be expected in pre-clinical small animal studies utilizing ^{67}Cu , phantom imaging was performed on a Siemens Inveon PET/SPECT/CT system using a Derenzo-style phantom, which consists of activity-filled rods separated by a distance that is twice the diameter of each rod in a tightly-packed triangular configuration. The decreasing diameters of each series of rods informs of the resolving power of a given imaging system (Cox *et al* 2016). Images were acquired using the mouse medium energy (MME) single pinhole collimation (3 mm). Prior to scan acquisition, system calibration was performed using a small amount of activity 925 kBq (25 μCi) of ^{67}Cu in the center of the detector field of view within a fillable spherical phantom with a volume of 0.250 ml. This acquisition was performed over a period of 10 h, which allowed for automated detector energy-response characterization and intrinsic flood calibration. Following calibration, the Derenzo phantom was filled with 16.6 MBq (0.449 mCi) of ^{67}Cu and scan acquisition was completed (90 projections, 30 s per projection). Scans were then reconstructed by 3D ordered subset expectation maximization (OSEM3D, 8 iterations, 6 subsets).

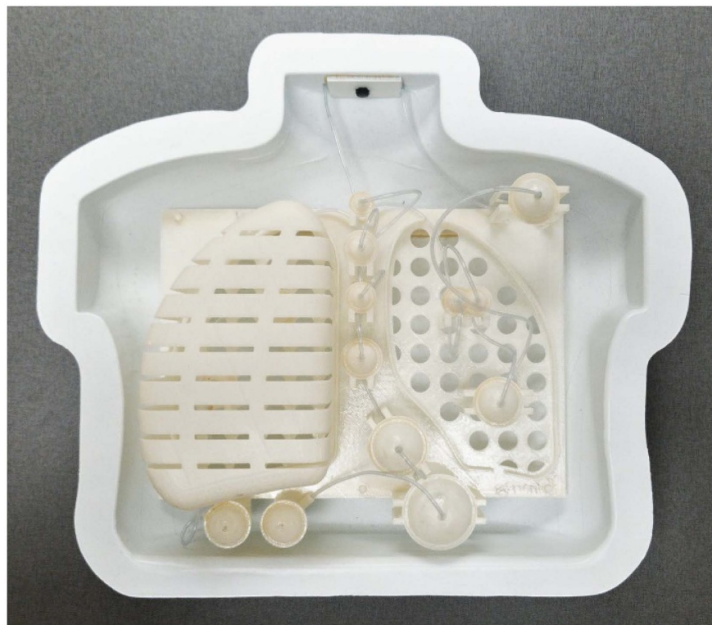


Figure 2. Society for Nuclear Medicine and Molecular Imaging (SNMMI) Clinical Trials Network (CTN) anthropomorphic chest phantom. NEMA sized spherical ‘tumors’ can be filled independent of the background. Styrofoam objects are used to displace activity within the lung regions, simulating an average lung tissue density of $\sim 0.45 \text{ g cc}^{-1}$.

Table 1. Summary image acquisition specifications.

Radionuclide	Image Acquisition Specifications
^{67}Cu	Siemens Intevo SPECT/CT, Activity: 222 MBq (6 mCi), 120 projections, 60 projections/head, 20 s/projection, 128×128 matrix, 15% energy window around photopeak, 15% scatter window below photopeak, ME collimator, reconstructed using MIM SPECTA Quant 6i10s
$^{99\text{m}}\text{Tc}$	Siemens Intevo SPECT/CT, Activity: 777 MBq (21 mCi), 120 projections, 60 projections/head, 15 s/projection, 128×128 matrix, 15% energy window around photopeak, 15% scatter window below photopeak, LEHR collimator, reconstructed using MIM SPECTA Quant 6i10s
^{177}Lu	Siemens Intevo SPECT/CT, Activity: 1.18 GBq (32 mCi), 120 projections, 60 projections/head, 15 s per projection, 128×128 matrix, 15% energy window around photopeak, 15% scatter window below the photopeak, ME collimator, reconstructed using MIM SPECTRA Quant 6i10s
^{64}Cu	GE Discovery MI PET/CT, Activity: 370 MBq (10 mCi), 10 min per bed position, reconstructed using Siemens VPFX 4i16s

2.6. Clinical SPECT/CT imaging

To evaluate the imaging characteristics of ^{67}Cu in a clinical setting, phantom imaging was performed on a clinical SPECT/CT system (Siemens Intevo). An anthropomorphic chest phantom (SNMMI CTN3 phantom figure 2), containing NEMA-sized spherical ‘tumors’ (7–37 mm), was filled with a tumor-to-background ratio of 5:1. These results were then qualitatively compared against similar images obtained for $^{99\text{m}}\text{Tc}$, ^{177}Lu , and ^{64}Cu . Acquisitions and reconstructions were completed as described in table 1. Recovery coefficients were then calculated using equation (1), where A_{meas} is the measured activity with a given sphere obtained using MIM imaging software and A is the actual administered activity to the same sphere. Additionally, the tumor-to-background ratio is verified at this time, as an additional verification for correct dose administration.

$$RC = \frac{A_{\text{meas}}}{A} \quad (1)$$

2.7. Dosimetric evaluation of ^{67}Cu

To evaluate the potential dosimetric characteristics of ^{67}Cu , Monte Carlo simulations were performed to obtain dose point kernels for ^{67}Cu and other clinically relevant beta emitting particles. Nuclear data was obtained from the National Nuclear Data Center, based on that data, isotropic point sources of radioactivity

Table 2. Summary of relevant beta-emitting radioisotopes.

Radionuclide	⁶⁷ Cu	¹³¹ I	⁹⁰ Y	¹⁷⁷ Lu	¹⁶⁶ Ho	¹⁸⁶ Re
Half-Life	61.8 h	8.03 d	64.1 h	6.64 d	26.8 h	3.72 d
Mean β^- Energy	141 keV (100%)	182 keV (100%)	934 keV (100%)	134 keV (100%)	665 keV (100%)	347 keV (93%)
Principle Gamma Energy	185 keV (49%)	606 keV (90%)	—	208 keV (10%)	1774 keV (50%)	1070 keV (71%)

Table 3. ⁶⁷Cu branching ratio measurements obtained by normalizing to the emission rate of the principle gamma (184.7 keV) in comparison with literature ⁶⁷Cu branching ratios (Huo *et al* 2005).

Energy Peak (keV)	Measured BR (Normalized to literature 184.7 keV)	Cu-67 Literature BR
91.4	7.68% \pm 0.59%	7.00% \pm 0.10%
93.5	17.43% \pm 1.31%	16.10% \pm 0.20%
184.7	—	48.7% \pm 0.3%
209.0	0.11% \pm 0.01%	0.115% \pm 0.005%
300.2	0.82% \pm 0.06%	0.797% \pm 0.011%
393.4	0.22% \pm 0.02%	0.220% \pm 0.008%

in water were simulated using Monte Carlo N-Particle transport (MCNP) v6.2 (Graves *et al* 2019). Simulations were performed with energy deposition being tallied in spherical shells out to a maximum radius of 2 meters. The simulations consisted of one million particles transported for each radiation mode of each radionuclide. General decay characteristics of beta-emitting radioisotopes that were simulated within MCNP are listed in table 2. Pharmacokinetic parameters for the common therapeutic radiopharmaceutical ¹⁷⁷Lu-DOTATATE—obtained from literature (Levart *et al* 2019, Lubberink *et al* 2020)—were used in conjunction with the physical half-life and energy emitted per decay to estimate the necessary clinically administered activity of ⁶⁷Cu. The rationale for using ¹⁷⁷Lu-DOTATATE for our pharmacokinetic comparison is due recent FDA approval of ⁶⁴Cu-DOTATATE, so it is not unlikely that ⁶⁷Cu-DOTATATE could be produced and used clinically. It is certainly possible that the chemical difference between the two could significantly impact the pharmacokinetics and therefore the administered activities. However, we feel that providing this initial estimate could be helpful to future investigations.

3. Results

3.1. ⁶⁷Cu production

A total of 62.9 GBq (1.7 Ci) of ⁶⁷Cu was produced within the isotopically-enriched metallic ⁶⁸Zn ingot over the irradiation period of 53.5 h. No short-lived radionuclidic impurities were detected by gamma spectroscopy prior to transferring activity from Argonne National Laboratory to the University of Iowa. The chemically isolated product appeared clear and colorless prior to evaporation for shipping. Good chemical purity was observed by ICP-MS and by effective molar activity titration (TETA: 0.88 Ci/ μ mol; DOTA 0.76 Ci/ μ mol; See supplemental material for details available online at stacks.iop.org/PMB/36/035002/mmedia).

3.2. Radionuclidic purity evaluation

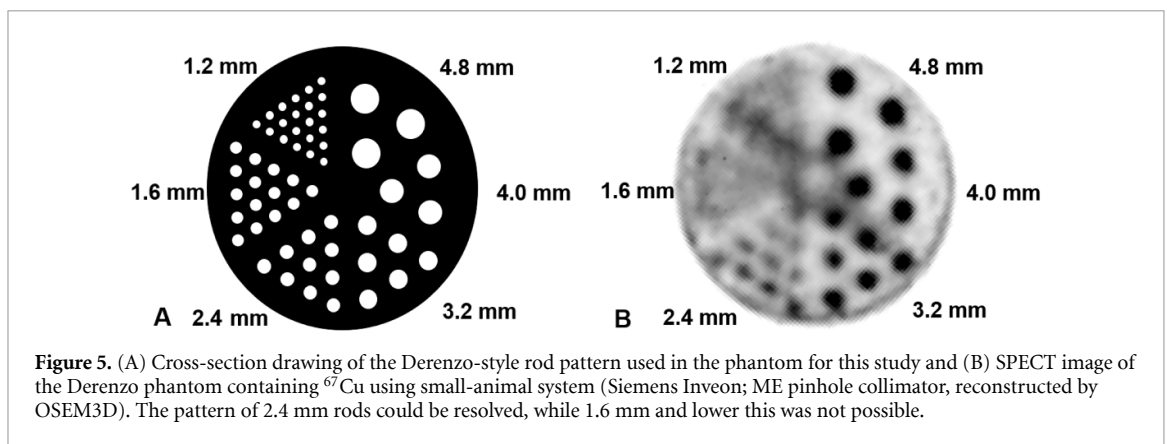
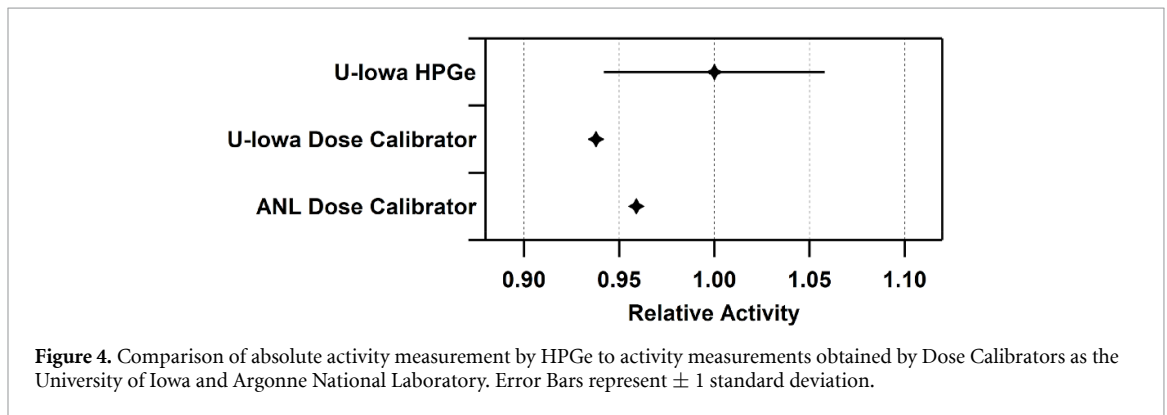
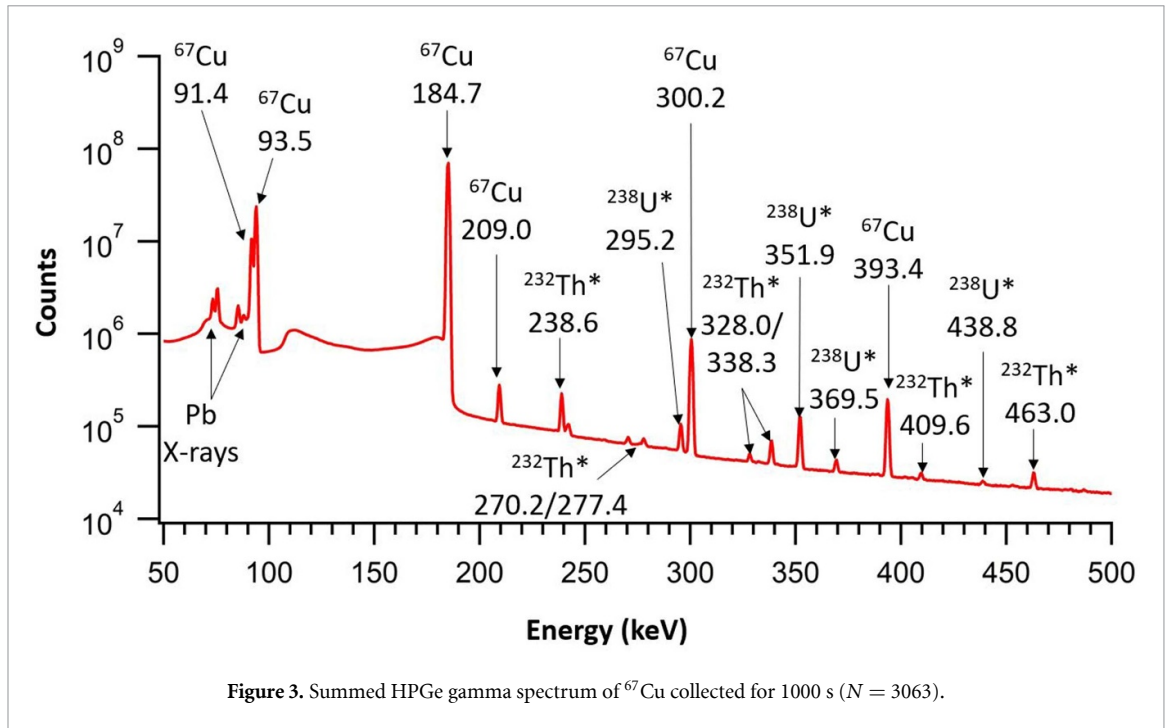
Following calibration of the HPGe detector, an acquisition was then acquired using a small known sample of ⁶⁷Cu (6.10 MBq/0.165 mCi) for 1000 s. Gamma spectrometry of ⁶⁷Cu is shown in figure 3. No impurities were detected, other than Pb x-rays due to the detector collimation and naturally occurring background radioisotopes. Branching ratios (BRs) measured for ⁶⁷Cu emission are listed in table 3. Measured branching ratios were consistent with literature values, suggesting the absence of ⁶⁷Ga.

3.3. Absolute activity verification and dose calibrator settings

With the use of the same data as above, absolute activity was determined through the analysis of each peak which was then converted into an absolute activity, again while incorporating propagated error analysis. Once this was completed for each individual peak, a weighted average was used to determine with greater accuracy the overall absolute activity and statistical uncertainty in the measurement (figure 4).

3.4. Pre-clinical μ SPECT/CT imaging

μ SPECT/CT images were obtained of the Derenzo phantom containing ⁶⁷Cu as described previously. Resulting image provided the smallest resolvable hole pattern of 2.4 mm using MME collimation (figure 5). Acquisition was attempted with Mouse Low Energy (MLE) collimation; however, no patterns could be resolved. Prior studies have demonstrated PET isotopes display slightly higher resolution results on the



Inveon MicroPET scanner, with ^{52}Mn (1.00 mm), ^{64}Cu (1.00 mm), ^{89}Zr (1.25 mm) and ^{124}I (1.50 mm) (Cox et al 2016). These results show that through SPECT imaging of ^{67}Cu we can obtain high quality images that can be obtained during/post treatment, which are not quite analogous to PET images, but do present the ability to resolve images which are adequate for tumor identification.

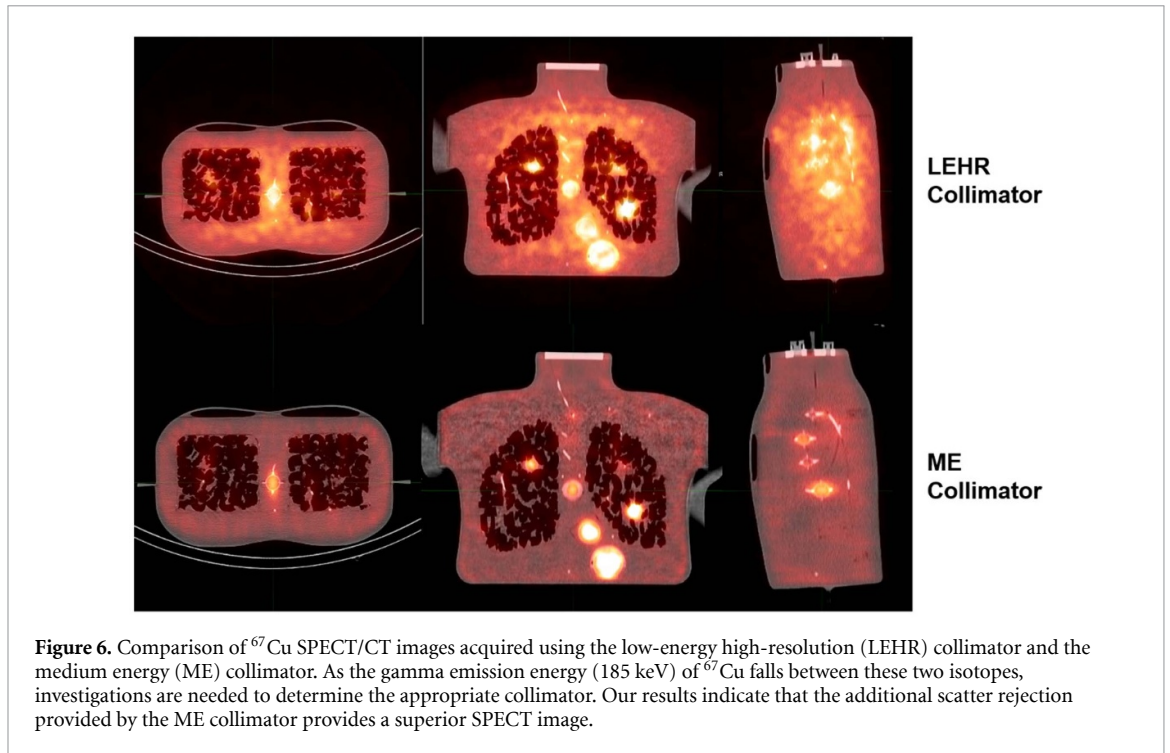


Figure 6. Comparison of ^{67}Cu SPECT/CT images acquired using the low-energy high-resolution (LEHR) collimator and the medium energy (ME) collimator. As the gamma emission energy (185 keV) of ^{67}Cu falls between these two isotopes, investigations are needed to determine the appropriate collimator. Our results indicate that the additional scatter rejection provided by the ME collimator provides a superior SPECT image.

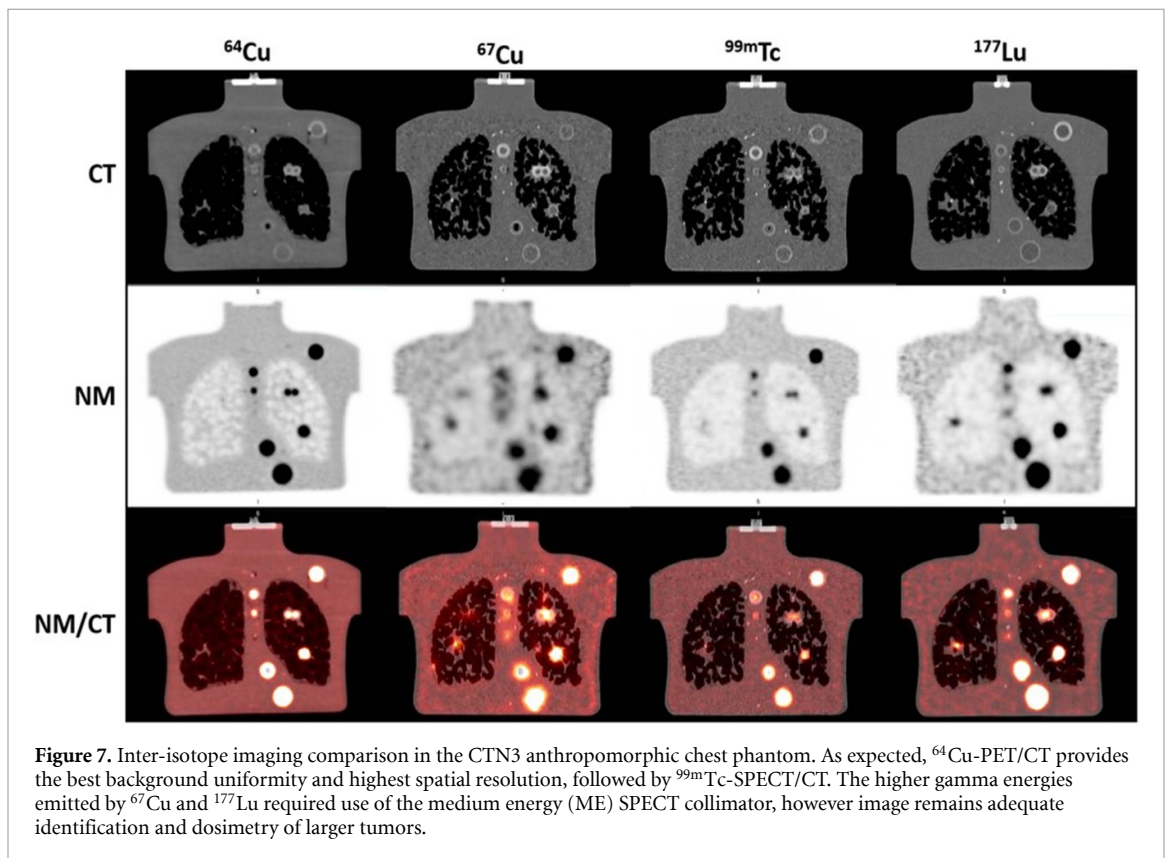


Figure 7. Inter-isotope imaging comparison in the CTN3 anthropomorphic chest phantom. As expected, ^{64}Cu -PET/CT provides the best background uniformity and highest spatial resolution, followed by $^{99\text{m}}\text{Tc}$ -SPECT/CT. The higher gamma energies emitted by ^{67}Cu and ^{177}Lu required use of the medium energy (ME) SPECT collimator, however image remains adequate identification and dosimetry of larger tumors.

3.5. Clinical SPECT/CT imaging

SPECT images of the SNMMI CTN3 phantom containing ^{67}Cu were obtained using both low-energy high-resolution (LEHR) collimator and the medium energy (ME) collimator. The LEHR collimator is typically used for $^{99\text{m}}\text{Tc}$ (140 keV), whereas the ME collimator is typically recommended for ^{177}Lu (208 keV) (Dewaraja *et al* 2012, Ljungberg *et al* 2016). The dominant gamma emission energy (185 keV) of ^{67}Cu falls between these two isotopes, thus investigation was necessary to determine the appropriate collimation. Results indicate that the reduced collimator septal penetration provided by the ME collimator yields significantly improved image quality compared with images acquired using LEHR collimation (figure 6).

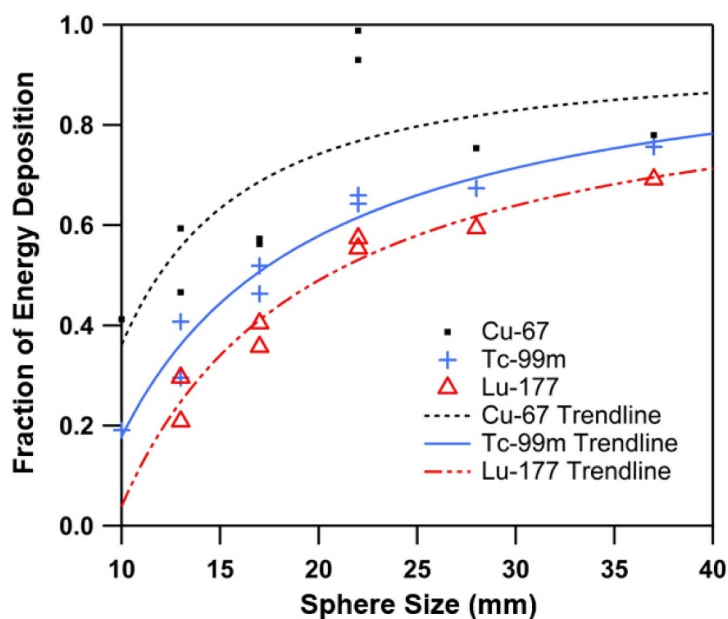


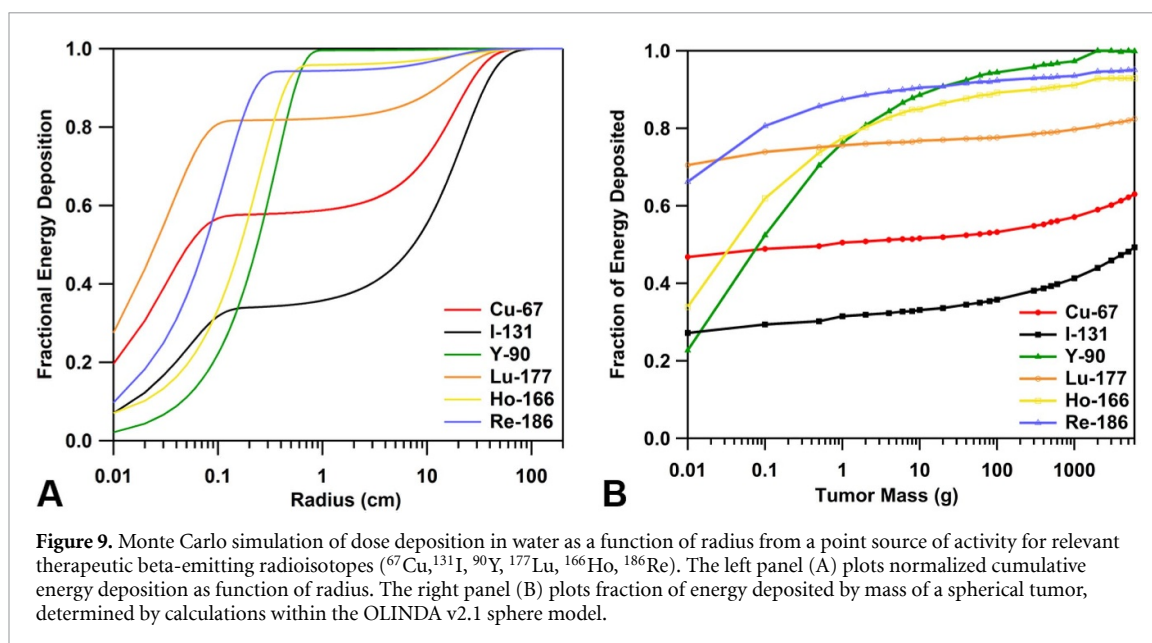
Figure 8. Recovery Coefficient Curves (RCCs) obtained using quantitative analysis of SPECT/CT images. ^{67}Cu RCC was obtained with a tumor to background ratio of 5:1. $^{99\text{m}}\text{Tc}$ and ^{177}Lu RCC were both obtained with a tumor to background ratio of 10:1.

Copper-67 SPECT images acquired using the ME collimator were compared to SPECT images obtained using $^{99\text{m}}\text{Tc}$ (LEHR collimator) and ^{177}Lu (ME collimator), and PET images obtained using ^{64}Cu . Through qualitative comparison we found that the PET image obtained using ^{64}Cu provides the best background uniformity and highest spatial resolution, followed by the $^{99\text{m}}\text{Tc}$ SPECT image. Next ^{67}Cu and ^{177}Lu have reduced image quality, however, image quality is still adequate for tumor identification (figure 7). This suggests that post-treatment dosimetry is possible for ^{67}Cu -bearing radiopharmaceuticals, as it is for ^{177}Lu (Dewaraja *et al* 2012, Ljungberg *et al* 2016). Somewhat higher noise levels are observable in the ^{67}Cu imaging, likely due to a lower level of activity (and comparably weaker counting statistics) within the phantom. Within the ^{67}Cu and ^{177}Lu NM images, apparent regional increases in activity concentration—particularly in the right lung—are attributable to partial volume effects from ‘tumors’ which are not included in the specific coronal slice that is shown in figure 7. From the known activity concentrations in each phantom, recovery coefficients were calculated for each isotope (figure 8). In terms of spatial resolution, ^{67}Cu would be expected to be equivalent to, or slightly greater than ^{177}Lu in terms of recovery coefficients, however the difference in our measurements was substantial, ostensibly due to the difference in tumor to background concentration ratios used for phantom filling.

3.6. Dosimetric characteristics of ^{67}Cu

Dose point kernels for ^{67}Cu , ^{131}I , ^{90}Y , ^{177}Lu , ^{166}Ho , and ^{186}Re produced by Monte Carlo simulations (MCNP 6.2), are shown in figure 9. These results allow for comparison of ^{67}Cu against other clinically relevant beta-emitting radioisotopes. On average, 57% of energy released during the decay of ^{67}Cu is absorbed within a sphere of radius 0.1 cm in water, whereas the remaining energy (primarily gamma emissions) is absorbed within a sphere of ~ 50 cm in water (figure 9(A)). In comparison with other isotopes, ^{67}Cu can be thought of as falling in-between ^{177}Lu and ^{131}I in terms of fractional energy released as photons, with similar beta particle ranges among the three isotopes.

Using the clearance rates available for ^{177}Lu -DOTATATE a clinically equivalent dose of ^{67}Cu was determined. Clearance rates were for 5, 24, 48, 96, 120 and 144 h, which show fractional remaining activity of 0.56, ~ 0.38 , 0.35, 0.17, 0.14 and 0.10 respectively (Levart *et al* 2019, Lubberink *et al* 2020). With this direct comparison, administration of 7.4 GBq (200 mCi) ^{177}Lu -DOTATATE was shown to be equivalent to approximately 10 GBq (270 mCi) of ^{67}Cu . However, it is important to note that this is a rough approximation, which assumes similar biodistribution and clearance to that of ^{177}Lu -DOTATATE, which may be altered by differing pharmacokinetics of ^{67}Cu and its designated chelator. In terms of radiation safety, the expected therapeutic level of ^{67}Cu will likely require more shielding than what is typically used for 200 mCi administrations of ^{177}Lu . This is due to the increased number of gamma emissions and shorter half-life. Copper-67 possesses a specific gamma-ray dose constant of 2.363×10^{-5} (mSv/h)/MBq, which is approximately 3 times greater than that of ^{177}Lu (7.636×10^{-6} (mSv/h)/MBq) (Unger and Trubey 1982).



Lutetium-177 is typically administered as an outpatient therapy, with minimal or no shielding while the patient is being infused, so this practice would need to be evaluated during the translation of ^{67}Cu -based radiopharmaceuticals and could warrant additional shielding and safety procedures.

4. Discussion

To our knowledge, this work constitutes the first reports of imaging performed using ^{67}Cu . These proof-of-principle imaging studies are a necessary and exciting step toward the potential clinical use of ^{67}Cu . Additionally, we have demonstrated the feasibility of producing ^{67}Cu in quantities and purities that are sufficient for undertaking preclinical and clinical therapeutic investigations. In addition to production logistics, based on our investigations, the imaging and dosimetric properties of ^{67}Cu appear suitable for oncologic applications.

Copper-67 is of interest for theranostic applications due to the isotope's physical traits, including half-life, decay schema and emission energies. The half-life of ^{67}Cu is approximately equal to the widely utilized therapeutic beta-emitting radioisotope ^{90}Y , however the average beta energy released per decay is significantly less (^{67}Cu : 141 keV; ^{90}Y : 934 keV). This leads to a shorter range in tissue, as illustrated by figure 9. It is also clear that ^{67}Cu lies between ^{177}Lu and ^{131}I in terms of relative dose from beta and photon emissions. Additionally, ^{67}Cu is the therapeutic pair to ^{64}Cu , a well-established clinically available PET isotope, this pairing is what will enable future theranostic applications of ^{67}Cu . Implementation of $^{64}\text{Cu}/^{67}\text{Cu}$ as a theranostic pair is consistent with the movement towards personalized radiopharmaceutical therapy, where ^{64}Cu patient specific pharmacokinetics can be observed and then used for therapeutic treatment planning for ^{67}Cu . These applications will be aided even further due to the established bioconjugate chemistry already available for ^{64}Cu (Moi *et al* 1985, Linder and Hazegh-Azam 1996, Lewis *et al* 1999a, 1999b, Bass *et al* 2000, Anderson and Ferdani 2009).

In regards to the radionuclidic purity of ^{67}Cu produced by the $^{68}\text{Zn}(\lambda, p)$ reaction, no impurities were detected. Of note is the potential difficulty in detecting a potential ^{67}Ga impurity by conventional gamma spectrometry, due to overlapping emission energies. For this reason, we have measured the emission branching ratios of ^{67}Cu samples by efficiency-calibrated HPGe. Results were in agreement with literature branching ratios for ^{67}Cu , indicating no significant ^{67}Ga impurity, as expected for this nuclear production route.

In evaluating the quantitative performance of dose calibrators for use with ^{67}Cu , we noted a systematic deviation of $\sim 5\%$ [68% C.I.: 0.94, 1.06] between values indicated by the dose calibrators and our absolute activity measurement by calibrated HPGe spectrometry. A true deviation of this magnitude would be clinically relevant, however improved absolute activity measurement precision will be needed to elucidate whether this effect is real. One way to reduce measurement error would be by the use of more appropriate standardized sources for calibration. Our current calibration protocol employs ^{152}Eu , ^{241}Am , ^{137}Cs , ^{57}Co and ^{60}Co , which leaves the major ^{67}Cu gamma peak of 185 keV poorly covered, thus resulting in increased

uncertainty in our detection efficiency. In future investigations, we intend to include a standardized source of $^{166\text{m}}\text{Ho}$ (E_{γ} : 184.4 keV, commercially available), as the emission energy is ideal for this particular application.

Initial quantitative imaging of ^{67}Cu demonstrates the feasibility of obtaining high-quality SPECT images from the dominant gamma emission of 185 keV. From the images obtained for ^{67}Cu it was determined that the produced images are adequate for identification of lesions as small as 10 mm with tumor to background concentration ratios of 5:1. As shown in figure 7, SPECT/CT of ^{67}Cu using ME collimation yields images that are qualitatively comparable to what is obtained using ^{177}Lu (208 keV, 10%). On a small animal imaging system with pin-hole based collimation, spatial resolution was substantially improved over what was observed on clinical imaging systems. Overall, our imaging experiments have yielded results that are consistent with what would be expected, given the decay scheme for ^{67}Cu .

A limitation of our comparison of ^{67}Cu to other isotopes was the difference in phantom fill conditions used for SPECT imaging, including total activity and tumor-to-background ratio. In future studies, care should be taken to utilize identical tumor-to-background ratios, and SPECT images should be acquired with the same total number of counts to minimize differences in image noise and spatial resolution. While our produced RC curve still shows the proof of concept of use for quantitative imaging, the difference may explain the slight variation between the compared isotopes. Another artifact within our RC curve calculation, is the 2 skewed points for the 22 mm spheres. This appears to be present due to the noise characteristics of the acquired scan and resolution recovery behavior of the iterative reconstruction. A repeated scan with a higher count density was attempted to verify this finding, however, our activity had precipitated from our solution by that time. Copper-67 was precipitation of activity was observed at late time-points, beyond 2–3 h post-filling, which was likely due to the instability of the Cu-DTPA complex. In future experiments, we intend to use more chelates with better stability for Cu (e.g. TETA or NOTA) to prevent precipitation and allow for longer scanning protocols.

Current production methods implemented at Argonne National Laboratory yield >62.9 GBq (1.7 Ci) of ^{67}Cu at end of bombardment, depending on irradiation time. This production yield is adequate for initiation of pre-clinical and clinical theranostic studies, with up to several therapeutic patient doses. Newer radiopharmaceutical designs have attempted to deliver similar therapeutic doses with lower levels of administered activity—via increased blood protein binding, increasing circulation time—which could drastically increase the number of patients treated from each ^{67}Cu production batch (Zang *et al* 2020).

7. Conclusion

Copper-67 possesses imaging and dosimetric characteristics that are similar to clinically available theranostic radioisotopes. This work confirms that new production methodologies enable high purity ^{67}Cu , suitable for clinical investigation.

Acknowledgments

This research is supported by the U.S. Department of Energy Isotope Program, managed by the Office of Science for Isotope R&D and Production.

Conflicts of interest

The authors have no conflicts of interest to disclose.

ORCID iDs

Michael J Merrick  <https://orcid.org/0000-0002-7803-9621>

David A Rotsch  <https://orcid.org/0000-0002-7184-9875>

Stephen A Graves  <https://orcid.org/0000-0003-2732-3064>

References

- Aarnio P, Nikkinen M and Routti J 1995 Gamma spectrum analysis including NAA with SAMPO for windows *J. Radioanal. Nucl. Chem.* **193** 179–85
- Aarnio P, Nikkinen M and Routti J 2001 UNISAMPO, comprehensive software for gamma-spectrum processing *J. Radioanal. Nucl. Chem.* **248** 371–5
- Anderson C J and Ferdani R 2009 Copper-64 radiopharmaceuticals for PET imaging of cancer: advances in preclinical and clinical research *Cancer Biother. Radiopharm.* **24** 379–93
- Bass L A, Wang M, Welch M J and Anderson C J 2000 In vivo transchelation of copper-64 from TETA-octreotide to superoxide dismutase in rat liver *Bioconjug. Chem.* **11** 527–32

- Cox B L, Graves S A, Farhoud M, Barnhart T E, Jeffery J J, Eliceiri K W and Nickles R J 2016 Development of a novel linearly-filled Derenzo microPET phantom *Am. J. Nucl. Med. Mol. Imaging* **6** 199–204
- Dasgupta A, Mausner L and Srivastava S 1991 A new separation procedure for ^{67}Cu from proton irradiated Zn *Int. J. Rad. Appl. Instrum. A* **42** 371–6
- Dewaraja Y K, Frey E C, Sgouros G, Brill A B, Roberson P, Zanzonico P B and Ljungberg M 2012 MIRDO pamphlet no. 23: quantitative SPECT for patient-specific 3-dimensional dosimetry in internal radionuclide therapy *J. Nucl. Med.* **53** 1310–25
- Ehst D, Smith N, Bowers D and Makarashvili V 2012 *AIP Conf. Proc.* **150** 157–61
- Ehst D A and Bowers D L 2013 Methods for making and processing metal targets for producing Cu-67 radioisotope for medical applications U.S. Patent No. US8526561B2
- Ehst D A and Willit J L 2016 Methods for producing Cu-67 radioisotope with use of a ceramic capsule for medical applications U.S. Patent No. US9312037B2
- Forrer F, Valkema R, Kwekkeboom D J, de Jong M and Krenning E P 2007 Peptide receptor radionuclide therapy *Best Pract. Res. Clin. Endocrinol. Metab.* **21** 111–29
- Graves S A, Flynn R T and Hyer D E 2019 Dose point kernels for 2,174 radionuclides *Med. Phys.* **46** 5284–93
- Grozinsky-Glasberg S and Gross D 2012 New drugs in the therapy of neuroendocrine tumors *J. Endocrinol. Invest.* **35** 930–6
- Huo J, Huang X and Tuli J 2005 Nuclear data sheets for $A=67$ *Nucl. Data Sheets* **106** 159–250
- Kaltsas G, Papadogias D, Makras P and Grossman A 2005 Treatment of advanced neuroendocrine tumours with radiolabelled somatostatin analogues *Endocr. Relat. Cancer* **12** 683–99
- Levart D, Kalogianni E, Corcoran B, Mulholland N and Vivian G 2019 Radiation precautions for inpatient and outpatient ^{177}Lu -DOTATATE peptide receptor radionuclide therapy of neuroendocrine tumours *EJNMMI Phys.* **6** 7
- Lewis J S, Lewis M R, Srinivasan A, Schmidt M A, Wang J and Anderson C J 1999a Comparison of four ^{64}Cu -labeled somatostatin analogues in vitro and in a tumor-bearing rat model: evaluation of new derivatives for positron emission tomography imaging and targeted radiotherapy *J. Med. Chem.* **42** 1341–7
- Lewis J S, Srinivasan A, Schmidt M A and Anderson C J 1999b In vitro and in vivo evaluation of ^{64}Cu -TETA-Tyr3-octreotate. A new somatostatin analog with improved target tissue uptake *Nucl. Med. Biol.* **26** 267–73
- Linder M C and Hazegh-Azam M 1996 Copper biochemistry and molecular biology *Am. J. Clin. Nutr.* **63** 797S–811S
- Ljungberg M, Celler A, Konijnenberg M W, Eckerman K F, Dewaraja Y K and Sjögren-Gleisner K 2016 MIRDO pamphlet no. 26: joint EANM/MIRD guidelines for quantitative ^{177}Lu SPECT applied for dosimetry of radiopharmaceutical therapy *J. Nucl. Med.* **57** 151–62
- Lubberink M, Wilking H, Öst A, Ilan E, Sandström M, Andersson C, Fross-Baron K, Velikyan I and Sundin A 2020 In vivo instability of ^{177}Lu -DOTATATE during peptide receptor radionuclide therapy *J. Nucl. Med.* **61** 1337–40
- Marceau N, Kruck T, McConnell D and Aspin N 1970 The production of copper 67 from natural zinc using a linear accelerator *Int. J. Appl. Radiat. Isot.* **21** 667–9
- Mitra E S 2018 Neuroendocrine tumor therapy: ^{177}Lu -DOTATATE *Am. J. Roentgenol.* **211** 278–85
- Moi M K, Mearns C F, McCall M J, Cole W C and Denardo S J 1985 Copper chelates as probes of biological systems: stable copper complexes with a macrocyclic bifunctional chelating agent *Anal. Biochem.* **148** 249–53
- Routti J T 1969 SAMPO, a Fortran IV program for computer analysis of gamma spectra from Ge (Li) detectors, and for other spectra with peaks No. UCRL-19452 (Berkeley, CA: Ernest Orlando Lawrence Berkeley National Laboratory) (<https://doi.org/10.2172/878125>)
- Schwarzbach R, Zimmermann K, Bläuenstein P, Smith A and Schubiger P A 1995 Development of a simple and selective separation of ^{67}Cu from irradiated zinc for use in antibody labelling: a comparison of methods *Appl. Radiat. Isot.* **46** 329–36
- Sun X and Anderson C J 2004 Production and applications of copper-64 radiopharmaceuticals *Methods in Enzymology* vol 386 (Amsterdam: Elsevier) pp 237–61
- Unger L and Trubey D K 1982 Specific gamma-ray dose constants for nuclides important to dosimetry and radiological assessment No. ORNL/RSIC-45/Rev. 1 (Oak Ridge, TN: Oak Ridge National Lab) (<https://doi.org/10.2172/5158466>)
- Zang J, Liu Q, Sui H, Wang R, Jacobson O, Fan X, Zhu Z and Chen X 2020 ^{177}Lu -EB-PSMA radioligand therapy with escalating doses in patients with metastatic castration-resistant prostate cancer *J. Nucl. Med.* **61** 1772–8